

Multi-scale order recurrence quantification analysis of EEG signals evoked by manual acupuncture in healthy subjects

Guosheng Yi · Jiang Wang · Hongrui Bian ·
Chunxiao Han · Bin Deng · Xile Wei ·
Huiyan Li

Received: 23 April 2012 / Revised: 25 July 2012 / Accepted: 17 September 2012 / Published online: 26 September 2012
© Springer Science+Business Media Dordrecht 2012

Abstract To explore the effects of manual acupuncture (MA) on brain activities, we design an experiment that acupuncture at acupoint ST36 of right leg with four different frequencies to obtain electroencephalograph (EEG) signals. Many studies have demonstrated that the complexity of EEG can reflect the states of brain function, so we propose to adopt order recurrence quantification analysis combined with discrete wavelet transform, to analyze the dynamical characteristics of different EEG rhythms under acupuncture, further to explore the effects of MA on the complexity of brain activities from multi-scale point of view. By analyzing the complexity of five EEG rhythms, it is found that the complexity of delta rhythm during acupuncture is lower than before acupuncture, and for alpha rhythm that is higher, but for beta, theta and gamma rhythms there are no obvious changes. All of those effects are especially obvious during acupuncture with frequency of 200 times/min. Furthermore, the determinism extracted from delta, alpha and gamma rhythms can be regarded as a characteristic parameter to distinguish the state acupuncture at 200 times/min and the state before acupuncture. These results can provide a theoretical support for selecting appropriate acupuncture frequency for patients in clinical,

and the proposed methods have the potential of exploring the effects of acupuncture on brain activities.

Keywords Manual acupuncture · ST36 · EEG · ORQA · Complexity

Introduction

Acupuncture, an ancient therapeutic technique, is currently gaining popularity as an important modality of alternative and complementary of medicine, which has gradually recognized by the world through over 2,000 years clinical trails. A number of randomized clinical trials have shown its clinical effects in pain treatment and controlling stress, especially in the treatment of chronic pain syndromes, as proposed by NIH Consensus (NIH consensus conference 1998). There are different kinds of acupuncture, such as manual acupuncture (MA), electroacupuncture (EA) and magnetic stimulation. MA is one of the most popular treatments, which has many advantages, such as appropriate stimulus intensity, flexible operation skill and no side-effect (Han et al. 2010). Due to its public acceptance, increasing attentions are paid to explore the scientific explanation regarding the regulation and action mechanism of acupuncture. Previous clinical and experimental studies have indicated that most acupuncture effects are mediated via the brain (Han et al. 1982; Stux and Hammerschlag 2001). Therefore, more and more basic neuroscience researches have been focused on the modulation of brain activities during acupuncture stimulation. However, the mechanism of the interaction between acupuncture and brain activity is still largely unknown, and how acupuncture modulates different brain rhythms is also unclear.

G. Yi · J. Wang (✉) · B. Deng · X. Wei
School of Electrical and Automation Engineering, Tianjin
University, No. 92 Weijin Road, Tianjin 300072, China
e-mail: jiangwang@tju.edu.cn

H. Bian
No. 707 Research Institute, China Shipbuilding Industry
Corporation, Tianjin 300131, China

C. Han · H. Li
School of Automation and Electrical Engineering, Tianjin
University of Technology and Education, Tianjin 300222, China

Non-invasive brain imaging techniques, such as electroencephalogram (EEG), functional magnetic resonance imaging (fMRI) and positron emission tomography (PET), provide the possible solutions to these problems (Ritter et al. 2009; Tyvaert et al. 2009; Zhang et al. 2004; Paraskeva et al. 2004; Onton et al. 2005). Compared with fMRI, EEG has higher temporal resolution and lower spatial resolution (Gevins 1998; Fisher et al. 1992), which can simultaneously record multi-channel neural electrical signals in different brain areas at the macroscopic level. A basic research in cognitive science is to deal with the study of the brain behavior after short, surprising stimuli, such as MA. EEG has the ability to measure such event related changes in the brain potentials which are also called event related potentials (ERPs) (Sutton et al. 1965). Therefore, a lot of researchers introduce EEG to investigate the effects of MA on brain activity recently (Bian et al. 2011; Hsu et al. 2011; Luo et al. 2012).

EEG can not only reflect the characteristics of brain activity itself, but also yield clues concerning the underlying associated neural dynamics (Rosso et al. 2006). It can be regarded as the activities of ensembles of generators producing oscillations in several frequency ranges. Michel et al. (1992) have demonstrated that EEG rhythms in different frequency range behave differently at different functional states, and they are functionally related to information processing and behavior. It has been shown that event related EEG rhythms can reveal the dynamics of cognitive function (Debener et al. 2006). Therefore, it could help interpret the effects of acupuncture on brain activity by characterizing different EEG rhythms evoked by MA. The common method to extract EEG rhythms is wavelet transform (WT). As an alternative frequency representation, WT has been proved to have many advantages. For example, with wavelets the time evolution of the frequency patterns can be followed with an excellent resolution. And WT does not require stationarity. Further, the multi-scale feature of WT allows that a signal can be decomposed into a number of frequency ranges, and each rhythm represents a particular coarseness of the signal under study (Kiymik et al. 2005). All of these advantages are crucial when analyzing non-stationary signals such as event related EEG rhythms, where all the interesting activities take place in fractions of a second.

The information processing in the brain is reflected by dynamical changes in electrical activity in time, frequency and space (Rosso et al. 2006), which can be measured by EEG. Therefore, the concomitant studies require methods capable of describing the qualitative and quantitative variation of EEG signals. Because EEG is non-stationary and stems from a highly nonlinear dynamical system, the nonlinear methods, derived from the theory of nonlinear dynamical systems, could capitalize on these properties and extract more informative features from EEG signals.

Through nonlinear analysis, many experiment results have shown that the complexity parameter extracted from EEG can reflect the functional state of brain (Stam et al. 1996; Lee et al. 2001). For example, it is found that the complexity of the EEG activity is relatively lower in quiet sleep and highest during wakefulness (Carrozzi et al. 2004). It is also found that the complexity of EEG is higher in seizure-free state than that in seizure state (Ouyang et al. 2008). What is more, Bian et al. have shown that MA at ST36 can increase the complexity of EEG signals, which can be regarded as a characteristic parameter to distinguish the states during acupuncture and before acupuncture (Bian et al. 2011). One of the most widely used methods to analyze EEG complexity is order recurrence quantification analysis (ORQA) (Groth 2005). The ORQA method based on the order recurrence plot (ORP) can not only describe the distribution character of the recursive state points, but also reveal more significant information during transitions in the brain processes due to the surprising stimuli and to distinguish ERPs between single electrodes (Marwan et al. 2007). So it is more appropriate to study the complexity of different EEG rhythms evoked by MA. To measure the complexity which quantifies the small-scale structures in ORP, several recurrence quantification measures are applied to analyze the ERPs data (Marwan and Meinke 2004). It has been shown that especially the measures determinism (*DET*) can be used for discrimination of the events on a single trial level, because it has high computational efficiency and strong robustness against non-stationarity (Marwan et al. 2007). Therefore, we adopt the *DET* measure based on ORQA method to analyze the acupuncture experiment signals, extract the complexity parameters from different EEG rhythms, and further explore the effects of acupuncture on brain activity.

The paper is organized as follows. In “**Materials and methods**” section, the experimental procedure of acupuncture and the corresponding nonlinear analysis methods are introduced. In “**Results**” section, the results and corresponding data analysis are presented. Finally, the conclusions are given. Overall, we adopt two nonlinear time series analysis methods, i.e. ORQA and DWT, to investigate the effects of MA on the complexity of different EEG rhythms. The results and the proposed method in our study will be useful to lay a foundation for revealing acupuncture mechanism.

Materials and methods

Subjects

Experiments are performed in eight right-handed healthy volunteers (age: 23–27 years; five males and three females), who are naive and had no or little experience with acupuncture. All the volunteers have no personal

history of neurologic or psychiatric disorders, and are not abusing alcohol or illicit drugs. Every subject is free from neurological active medication, or any other factor that may affect EEG activities. Our study is performed with the approval of the local ethics committee. All the subjects have been provided informed consent with the adequate understanding of the purpose and procedure of the study and their informed written consent is obtained according to the declaration of Helsinki.

Acupuncture stimulation and experimental design

In our experiment, we acupuncture at the acupoint ST36 (Zusanli) on the right leg, shown in Fig. 1a. ST36 is an important meridian on Stomach Meridians, which has many therapeutically beneficial effects, such as keeping calm and sedative, treating sleep disorders, controlling stress, handling dizziness insomnia and gastrointestinal diseases, treating neurological disorders, and so on. This meridian works effectively and has been widely applied in Traditional Chinese Medical acupuncture experiments (Han 2004). Acupuncture is administered manually by a single licensed acupuncturist with in clinical practice for over 25 years. Stainless steel needles used for ST36 are 0.2 mm in diameter and 40 mm in length.

During the whole procedure, all operations are conducted in a dimly lit room where the subjects lie in a soft bed and stay in peace and awake. There is no obvious electromyographic signal interruption during the whole process, in order to obtain as many artifacts-free EEG data as possible. The subjects are instructed to keep their eyes closed and to relax during the whole acupuncture procedure. Before acupuncture, all subjects have 10 min to relax. Then, the stainless steel needles are inserted into ST36 as deep as 10–20 mm and keep resting in place for 2 min (R1). The whole acupuncture process lasts for about 25 min for every subject, as shown in Fig. 1c. First, the subjects are acupunctured by using the twirling method to cause the needling sensation for 2 min (M1). The twisting is within a range of 90°–180° and at a frequency of about 50 times/min. After that, the needle is resting in place for 4 min (R2). And then this process iterates 3 times by the identical needle with different frequency. The acupuncture frequency is 100 times/min (M2), 150 times/min (M3) and 200 times/min (M4), respectively. Between different frequency needle manipulations, there are always 4 min for needle to be resting in place (R3, R4 and R5). In order to avoid the influence induced by the order of four frequencies acupuncture stimuli, the order is chosen randomly.

EEG recording and preprocessing

EEG signals' recording is completed by Neuroscan system using 20 Ag–AgCl electrodes, which are placed according

to the 10–20 international system, as shown in Fig. 1b. Reference electrodes are placed between A1 and A2, using earlobe as reference ground. The cut-off frequencies of the EEG amplifiers are set to 0.5 and 100 Hz. We record 20-channel EEG signals at a 250 Hz sampling rate from 20 scalp electrodes, which are channels Fp1, Fp2, F7, F3, Fz, F4, F8, T3, C3, Cz, C4, T4, T5, P3, Pz, P4, T6, O1, Oz and O2, respectively.

Five segments of EEG signals are recorded for each subject, which are 2 min before acupuncture (BA), acupuncture with frequency 50 times/min (M1), acupuncture with frequency 100 times/min (M2), acupuncture with frequency 150 times/min (M3) and acupuncture with frequency 200 times/min (M4), as shown in Fig. 1d. The state before acupuncture, viz., no acupuncture stimulus, is the control condition in our study. Then, we intercept the intermediate 80 s data from each EEG segment, which are free of signs of muscle artifact, eye movements and other artifacts. Thus, 5×80 -s EEG epochs are obtained for each subject. The EEG datasets are preprocessed by a 0.5–48 Hz band-pass digital filter, to further eliminate artifacts induced by residual Electromyography (EMG) activity and noise owing to the electrical mains.

Wavelet transform

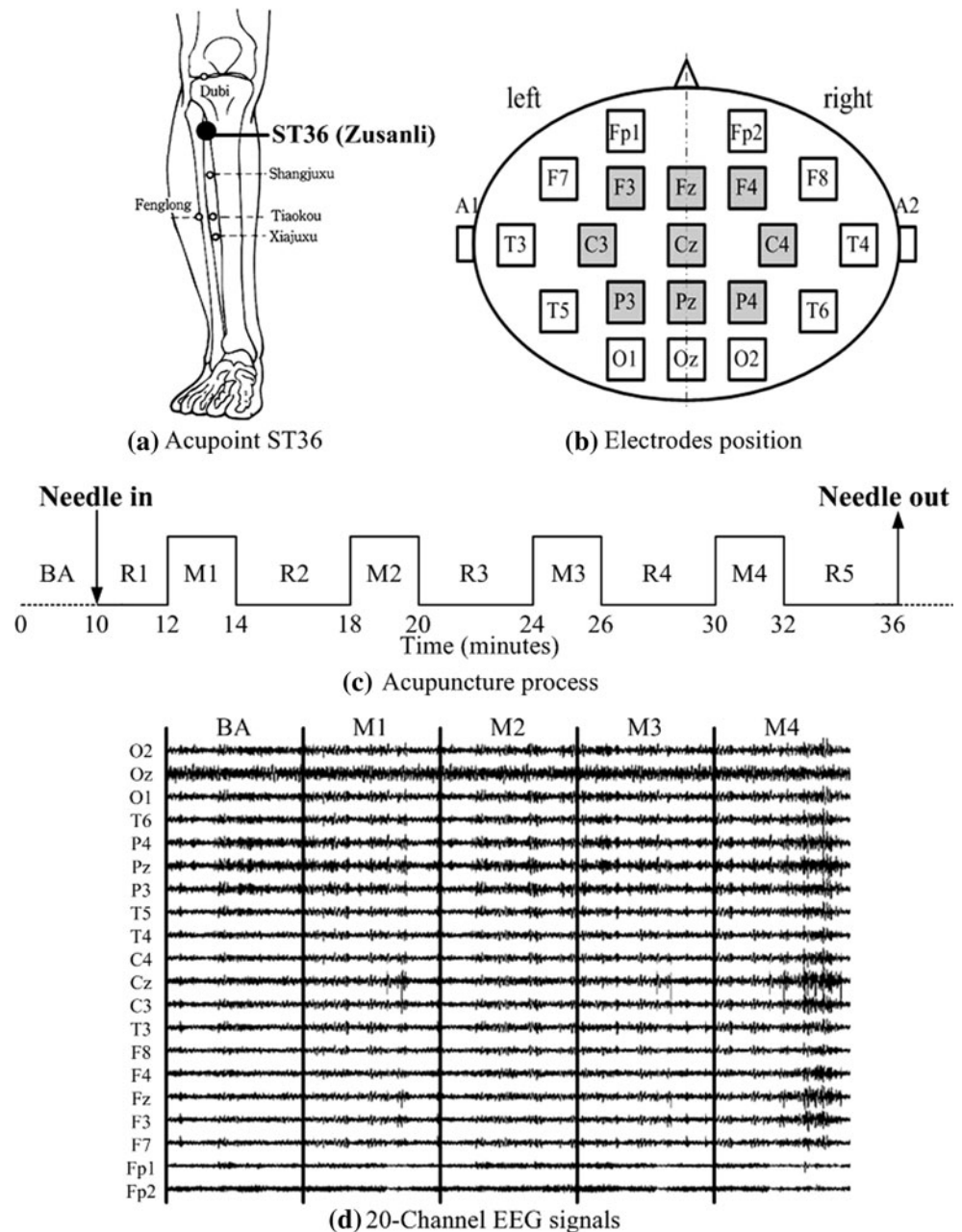
The wavelet analysis is a method which relies on the introduction of an appropriate basis and a characterization of the signal by the distribution of amplitude in the basis (Rosso et al. 2001). If the wavelet required can form a proper orthogonal basis, it has the advantage that an arbitrary function can be uniquely decomposed and the decomposition can be inverted (Aldroubi and Unser 1996; Mallat 1999). There are several types of wavelet transforms, such as continuous wavelet transform (CWT) and discrete wavelet transform (DWT). The CWT has two drawbacks: redundancy and impracticality, which can be solved by making discretize the transform parameters (Kiyimik et al. 2005).

The wavelet is a smooth and quickly vanishing oscillating function with good localization in both frequency and time. For a wavelet transform, the wavelet family $\psi_{a,b}(t)$ is the set of elementary functions generated by dilations and translations of a unique admissible mother wavelet $\psi(t)$, which is defined by:

$$\psi_{a,b}(t) = |a|^{-\frac{1}{2}} \psi\left(\frac{t-b}{a}\right) \quad (1)$$

where $a, b \in \mathbb{R}$, $a \neq 0$ are the scale and translation parameters respectively, and t is the time. As the scale parameter a increases, the wavelet becomes narrower. Thus, every specific wavelet transform has a unique analytic pattern and its replications at different scales and with variable

Fig. 1 Acupuncture experiment. **a** MA is administered to the ST36 (Zusanli) acupoint (Zusanli) on the right leg. **b** Electrodes position on brain. **c** Acupuncture process. All the subjects have 10 min to relax before acupuncture (BA). Then, the stainless steel needles are inserted into ST36 as deep as 10–20 mm. After remaining in place for 2 min (R1), the needle is twirled within a range of 90° – 180° for 2 min (M1) at a rate of about 50 times/min. After that, the needle is resting in place for 4 min (R2). Then this process iterates 3 times by the identical needle with different frequency. The acupuncture frequency is 100 times/min (M2), 150 times/min (M3) and 200 times/min (M4), respectively. Between different frequency needle manipulations, there are always 4 min for needle to be resting in place (R3, R4 and R5). **d** 20-channel EEG signals evoked by acupuncture for one subject, which are 2 min before acupuncture (BA), acupuncture with 50 times/min (M1), acupuncture with 100 times/min (M2), acupuncture with 150 times/min (M3) and acupuncture with 200 times/min (M4), respectively



time localization. In the present work, we employ orthogonal cubic spline functions as mother wavelets. That is because the cubic spline functions are symmetric and combine in a suitable proportion smoothness with numerical advantages (Rosso et al. 2001). Now, they have become a recommendable tool for representing natural signals.

For the discrete set of parameters, $a = 2^{-j}$ and $b = 2^{-j}k$ with $j, k \in \mathbb{Z}$ (the set of integers), the wavelet family $\psi_{a,b}(t)$ in Eq. (1) can be expressed as:

$$\psi_{j,k}(t) = 2^{\frac{j}{2}} \psi(2^j t - k), \quad j, k \in \mathbb{Z} \quad (2)$$

which constitutes an orthonormal basis of the Hilbert space

$L^2(\mathbb{R})$ consisting of finite-energy signals. The DWT of a signal $S(t) \in L^2(\mathbb{R})$ is defined as the correlation between the function $S(t)$ with the discrete family wavelet $\psi_{j,k}$ for each j and k , as Eq. (3) shown:

$$(W_{\psi} S) \left(\frac{k}{2^j}, \frac{1}{2^j} \right) = 2^{\frac{j}{2}} \int_{-\infty}^{\infty} S(t) \psi^*(2^j t - k) dt = \langle S, \psi_{j,k} \rangle \quad (3)$$

where $\langle x, y \rangle$ stands inner product.

Then the discrete signal for $S(t) \in L^2(\mathbb{R})$ is assumed to be given by the sampled values $S = \{s_0(n), n = 1, 2, \dots, M\}$ with sampling time t_s . For simplicity, the

sampling rate is taken as $t_s = 1$. If the decomposition is carried out over all resolutions levels ($N = \log_2(M)$), then the wavelet expansion will be:

$$S(t) = \sum_{j=-N}^{-1} \sum_k C_j(k) \psi_{j,k}(t) = \sum_{j=-N}^{-1} r_j(t) \quad (4)$$

where $C_j(k) = \langle S, \psi_{j,k} \rangle$ are wavelet coefficients, which can be interpreted as the local residual errors between successive signal approximations at scales j and $j + 1$. $r_j(t)$ is the residual signal at scale j , which contains the information of the signal $S(t)$ corresponding to the frequencies $2^{j-1}\omega_s \leq |\omega| \leq 2^j\omega_s$.

Order recurrence quantification analysis (ORQA)

Order recurrence plot (ORP), defined as a recursive state according to order structure of state variables in the phase space. Given a one-dimensional time series $\{x(it)\}_{i=1:n}$ (t is sampling time interval, n is the total number of sampling points), the original phase space can be reconstructed by using the Taken's time delay method (Takens 1981) with embedding dimension m and delay time τ . The points in the m -dimensional phase space can be expressed as:

$$\mathbf{X}_k(\mathbf{t}) = (x(kt), x(kt + \tau), \dots, x(kt + (m-1)\tau)) \quad (5)$$

where $k = 1, 2, \dots, N$ and $N = n - (m-1) * \tau/t$. Thus, one can obtain N m -dimensional vectors.

To discuss the order structure of the time series, we define a recurrence by using the local order structure of a trajectory. Given a one-dimensional time series, let us start to compare $m = 2$ time instances. Two relations between $x(kt)$ and $x(kt + \tau)$ are possible, neglecting equality. We denote these relations as order patterns π and derive the symbol sequence:

$$\pi_k(t) = \begin{cases} 0, & x(kt) < x(kt + \tau) \\ 1, & x(kt) > x(kt + \tau) \end{cases} \quad (6)$$

with the scaling parameter τ . This parameter ensures that the points considered in forming the order pattern π do not show trivial dependencies. Therefore, it can be easily found that there are increase and decrease order patterns for $m = 2$. For $m = 3$, there are $m! = 6$ different order patterns in the triple $(x(kt), x(kt + \tau), x(kt + 2\tau))$ possible, again neglecting equality. The phase space is decomposed by three planes into six equivalent regions, as shown in Fig. 2 (Marwan et al. 2007). In general, the m components in $X_k(t) = (x(kt), x(kt + \tau), \dots, x(kt + (m-1)\tau))$ can form $m!$ different patterns. Tied ranks ($x(kt) = x(kt + \tau)$) are assumed to be rare and we also neglect them.

From these order patterns we form a new symbolic time series π_i , and define the order patterns recurrence plot (OPRP) as (Groth 2005):

$$R_{ij}(m) = \begin{cases} 0, & \pi_i \neq \pi_j \\ 1, & \pi_i = \pi_j \end{cases} \quad i, j = 1, 2, \dots, N \quad (7)$$

The binary values of R_{ij} can be simply visualized with the black (1) and white (0). Thereby, ORP can be formed. In order to further investigate the properties of ORP, a simple measure of complexity which quantifies the small-scale structures in ORP called determinism has been proposed. The determinism (*DET*) measure which is based on the diagonal lines, is defined as the ratio of recurrence points on the diagonal structures to all recurrence points, and is introduced as a determinism (or predictability) measure of the system. Its formulation is given below:

$$DET = \sum_{l=l_{\min}}^N P(l) / \sum_{i,j=1}^N R_{ij} \quad (8)$$

where $P(l)$ is the frequency distribution of the lengths l of the diagonal structures in ORP, and l_{\min} is the threshold of length, which excludes the diagonal lines formed by the tangential motion of a phase space trajectory. In present work, l_{\min} is fixed at 2. The higher the determinism measure of a signal, the lower the complexity is. Processes with stochastic behavior cause none or very short diagonals, corresponding to a lower *DET* and higher complexity, whereas deterministic processes cause longer diagonals and less single, isolated recurrence points, which corresponds to a higher *DET* and lower complexity.

Results

The wavelet multiresolution decomposition is used for decomposing the recorded EEG signals into different scale levels defined in agreement with the traditional frequency bands derived by the clinical EEG analysis. After a five octave wavelet decomposition (in accordance with the sampling rate of 250 Hz), the components of the following frequency bands are obtained: 63–125 Hz ($j = -1$), 31–62 Hz ($j = -2$, gamma), 16–30 Hz ($j = -3$, beta), 8–15 Hz ($j = -4$, alpha), 4–7 Hz ($j = -5$, theta) and the residues in the 0.5–3 Hz band ($r = -5$, delta). The

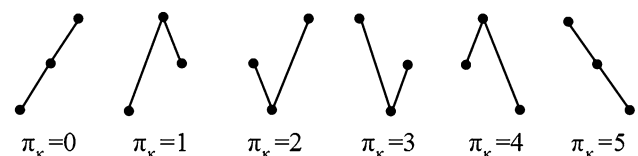
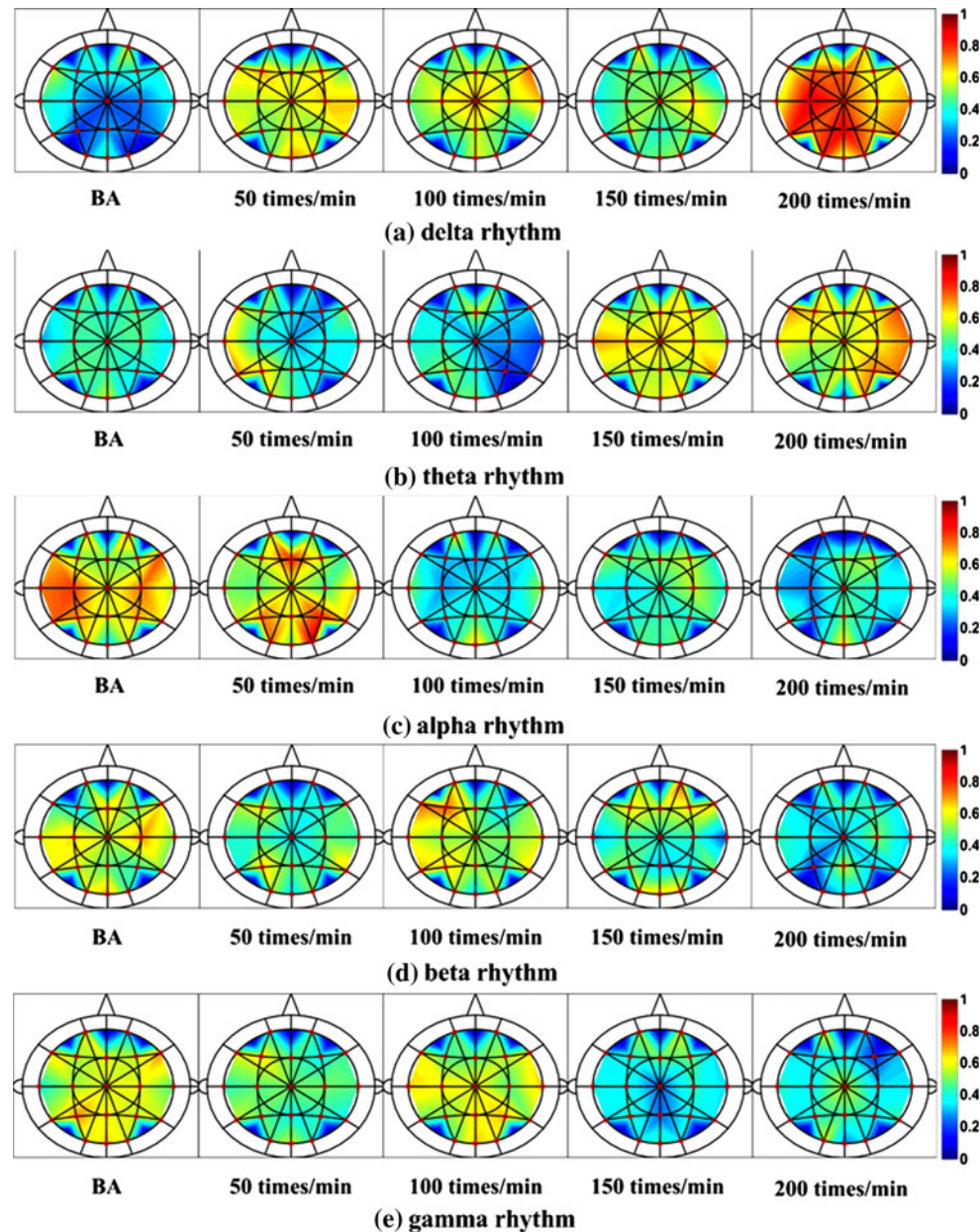


Fig. 2 Ordinal patterns for the dimension $m = 3$

Fig. 3 Brain electrical activity mapping of the *DET* values for delta (a), theta (b), alpha (c), beta (d) and gamma (e) rhythms at five different acupuncture states (BA stands for before acupuncture). The positions of the electrodes are indicated by small red dots and numbered according to the 10–20 electrode placement system shown in Fig. 1b. The color marks the *DET* values for five rhythms. Specifically, color towards red indicates an increase in the *DET* values, and color towards blue indicates a decrease



concrete step to compute *DET* is as follows. First, five EEG rhythms obtained by wavelet decomposition should be reconstructed into phase space by using the Taken's time delay method. The delay time τ and the embedding dimension m of entire EEG epochs are determined by using the self-correlation method and the false nearest neighbor (FNN) method, respectively. It is found that $\tau = 5$ and $m = 5$ is suitable for the topologically proper reconstruction of the EEG data. The moving windows of size 4 s with a shifting step of 1 s is applied to compute the *DET* for all EEG rhythms at five acupuncture states. Then, take the average value of *DET* over all moving windows. Therefore, the data of each EEG rhythm is transformed into a 20×5 matrix (20 channels \times 5 states) for every subject.

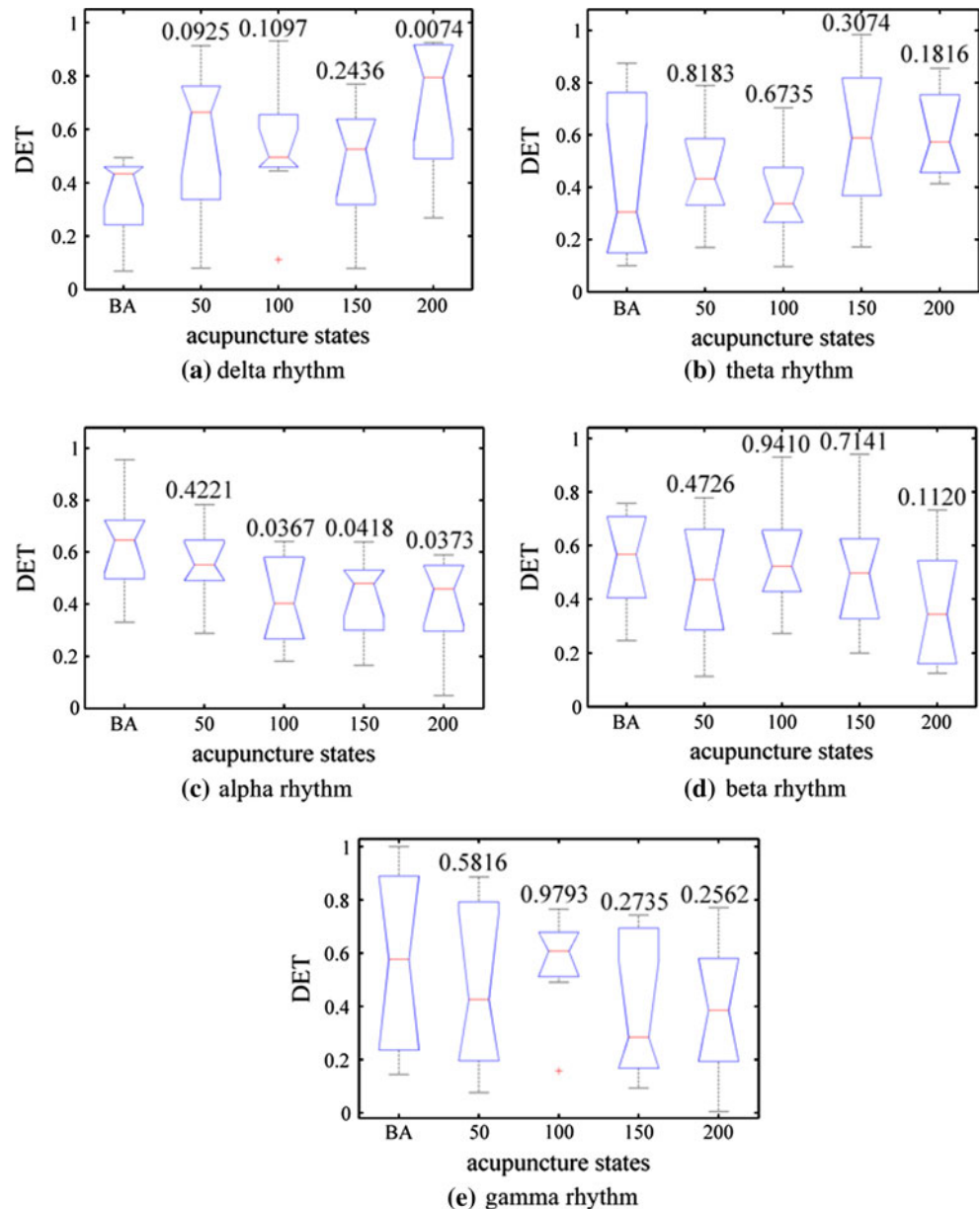
The results are normalized for the purpose of eliminating the influence of individual differences between different subjects. The normalization method is as follows. V_{Max} and V_{Min} represent the max and min element of 20×5 matrix respectively. $V(i, j)$ is the element in the matrix, with $1 \leq i \leq 20$, $1 \leq j \leq 5$, where i represents EEG channel and j represents the acupuncture state. $Vl(i, j)$ is the value in the normalized matrix and is calculated as follows:

$$Vl(i, j) = [V(i, j) - V_{\text{Min}}] / (V_{\text{Max}} - V_{\text{Min}}). \quad (9)$$

For every subject, a normalized matrix with values between 0 and 1 is obtained.

Taking the average value of normalized *DET* over eight subjects, brain electrical activity mapping of the average

Fig. 4 Box plot of the average *DET* values of 20 electrode sites at five different acupuncture states for delta (a), theta (b), alpha (c), beta (d) and gamma (e) rhythms (BA stands for the state before acupuncture). The *digital* marked in the figure are the probability level of *DET* during acupuncture compared with that before acupuncture. The *notches* in the boxes are a graphic confidence interval (95 %) about the median of a sample. The *lower* and *upper* lines of the box are the 25th and 75th percentiles of the sample, the distance between the *top* and *bottom* of the box is the inter quartile range and the *line* in the *middle* of the box is the sample median

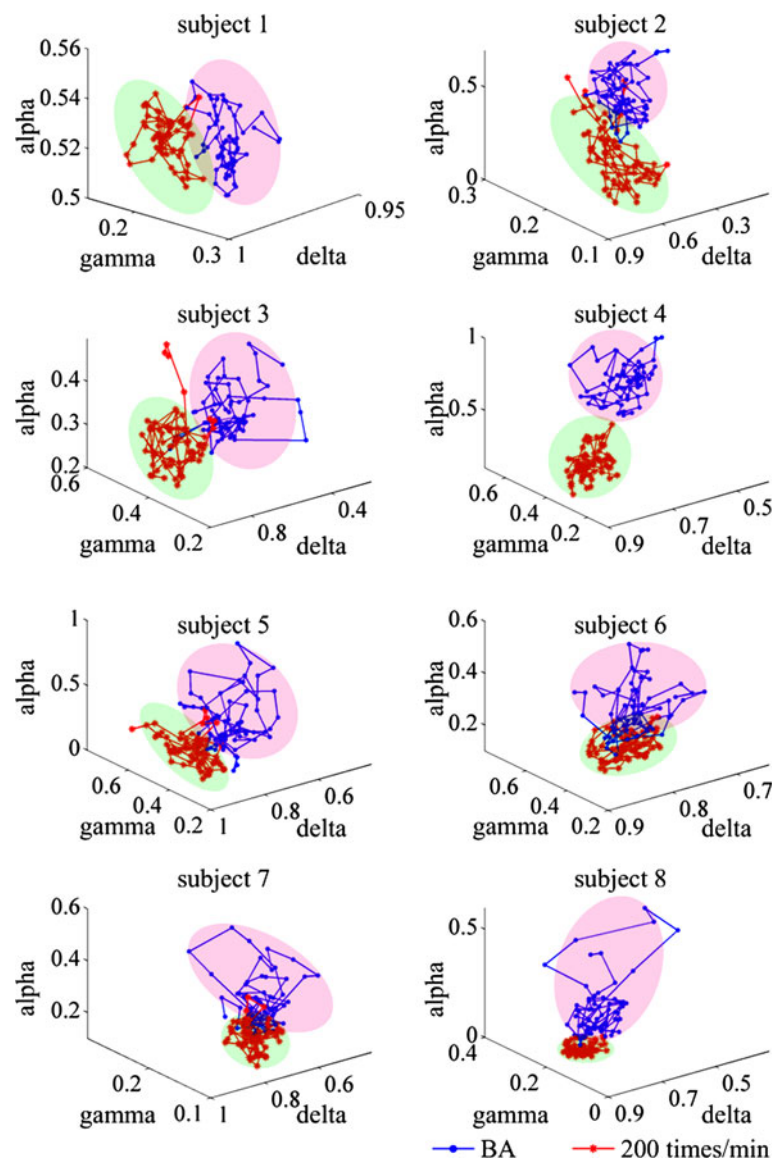


DET for each rhythm at five acupuncture states is shown in Fig. 3. Moreover, the average influence degree of acupuncture on the entire cerebral complexity is also studied by calculating the average value of *DET* over 20 electrode sites for each subject. Statistical analysis of the *DET* values in each state is carried out to determine whether their distributions between states before acupuncture and during acupuncture are significantly different. A one-way ANOVA is performed using standard tool of numerical analysis (Matlab's ANOVA routine, statistics toolbox). The results are presented in Fig. 4. The numbers marked in Fig. 4 are the probability level of *DET* at the corresponding acupuncture state compared with that before acupuncture.

As shown in Figs. 3a and 4a, the average *DET* of delta rhythm during acupuncture is higher than that before

acupuncture and especially during acupuncture with frequency of 200 times/min ($P = 0.0074$); In Figs. 3b and 4b, the average *DET* of theta rhythm during acupuncture with frequencies of 150 and 200 times/min is higher than that before acupuncture, but almost remain the same in frequencies of 50 and 100 times/min compared with that before acupuncture; As shown in Figs. 3c and 4c, the average *DET* of alpha rhythm during acupuncture is lower than that before acupuncture except in frequency of 50 times/min, which indicates that acupuncture makes the random element increase, i.e. complexity. The change of the average *DET* of beta rhythm during acupuncture is not obvious, except for the frequency of 200 times/min which decreases slightly, as shown in Figs. 3d and 4d. In Figs. 3e and 4e, the average *DET* of gamma rhythm in frequencies

Fig. 5 3D figures of the average *DET* in each moving window of alpha, gamma and delta rhythms at two states for eight subjects. The two states are before acupuncture (BA) and acupuncture at 200 times/min



of 50 and 100 times/min is almost the same as that before acupuncture, but decreases slightly in frequencies of 150 and 200 times/min. From the above, by using ORQA combined with DWT, we can draw the conclusion that acupuncture at ST36 has induced different effects on five basic EEG rhythms, especially on delta and alpha rhythms. Further, the effects of acupuncture on five EEG rhythms are most obvious when the acupuncture frequency is 200 times/min.

Besides, for alpha, gamma and delta rhythms, the average value of *DET* over all electrode sites is calculated in each moving window respectively. Then taking these average *DET* of three rhythms as coordinates, we can draw a 3D figure for each subject. For the states acupuncture at 200 times/min and before acupuncture, it can be found that the average *DET* of two states is mainly distributed in two different areas for all the subjects, as Fig. 5 shown.

Therefore, the average *DET* of all electrode sites extracted from alpha, gamma and delta rhythms can be regarded as a characteristic parameter to distinguish the state acupuncture at 200 times/min and the state before acupuncture.

Conclusions

To investigate the effects of MA on brain activity, we design an experiment that acupuncture at ST36 of right leg taken with four different frequencies to obtain EEG signals from eight subjects in this paper. As the complexity parameters extracted from different rhythms of EEG can reflect brain functional state, we propose to adopt two nonlinear time series analysis methods, i.e. ORQA and DWT, to investigate the effects of MA on the complexity of brain rhythms. The DWT method is used to decompose the recorded EEG

signals into different scale levels, which is in agreement with the traditional frequency bands derived by the clinical EEG analysis. Then, we analyze the nonlinear deterministic structure in five EEG rhythms at different acupuncture states by using the ORQA measure-*DET*, which is known as a determinism (predictability) measure of a dynamical system. The higher *DET* values imply that local neural networks become more predictable (less complex). To our knowledge, we are the first one to use ORQA to analyze the EEG signals evoked by MA for understanding the effects of acupuncture on different EEG rhythms. Further, we have verified the proposed methods in our study have the potential of exploring the effects of acupuncture on brain activities from multi-scale point of view.

Our results show that the complexity of delta rhythm during acupuncture is lower than that before acupuncture, while the complexity of alpha rhythm is higher than that before acupuncture. Besides, there is almost no obvious change in the complexity of theta, beta and gamma rhythms. Those effects are especially obvious during acupuncture with frequency of 200 times/min. Further, the *DET* extracted from alpha, gamma and delta rhythms can be regarded as a characteristic parameter of distinction between the state acupuncture at 200 times/min and the state before acupuncture. These results shed light on how MA modulates brain activity from multi-scale point of view. The nonlinear quantitative analysis of acupuncture signals can be used to make MA more standardized. All of these principles may guide future therapeutics to select appropriate acupuncture frequency for patients in clinical. They can provide a theoretical support for uncovering the regulation and action mechanism of the interactions between acupuncture and brain activity.

Acknowledgments This work was supported by the Key Program of the National Natural Science Foundation of China (Grant No. 50537030), the National Natural Science Foundation of China (Grant No. 61072012 and 61172009), the Young Scientists Fund of the National Natural Science Foundation of China (Grant No. 61104032 and 60901035).

References

- Aldroubi A, Unser M (1996) Wavelets in medicine and biology. CRC Press, Boca Raton
- Bian HR, Wang J, Han CX, Deng B, Wei XL, Che YQ (2011) Features extraction from EEG signals induced by acupuncture based on the complexity analysis. *Acta Phys Sin* 60(11):118701
- Carrozzi M, Accardo A, Bouquet F (2004) Analysis of sleep-stage characteristics in full-term newborns by means of spectral and fractal parameters. *Sleep* 27:1384–1393
- Debener S, Ullsperger M, Siegel M, Engel AK (2006) Single-trial EEG-fMRI reveals the dynamics of cognitive function. *Trends Cogn Sci* 10(12):558–563
- Fisher RS, Webber WR, Lesser RP, Arroyo S, Uematsu S (1992) High-frequency EEG activity at the start of seizures. *J Clin Neurophysiol* 9:441–448
- Gevins A (1998) The future of electroencephalography in assessing neurocognitive functioning. *Electroencephalogr Clin Neurophysiol* 106(2):165–172
- Groth A (2005) Visualization of coupling in time series by order recurrence plots. *Phys Rev E* 72(4 Pt 2):046220
- Han JS (2004) Acupuncture and endorphins. *Neurosci Lett* 361(1–3):258–261
- Han JS, Xie GX, Zhou ZF, Folkesson R, Terenius L (1982) Enkephalin and beta-endorphin as mediators of electro-acupuncture analgesia in rabbits: an antiserum microinjection study. *Adv Biochem Psychopharmacol* 33:369–377
- Han CX, Wang J, Che YQ, Deng B, Guo Y, Guo YM, Liu YY (2010) Nonlinear characteristics extraction from electrical signals of dorsal spinal nerve root evoked by acupuncture at Zusanli point. *Acta Phys Sin* 59(8):5881–5888
- Hsu SF, Chen CY, Ke MD, Huang CH, Sun YT, Lin JG (2011) Variations of brain activities of acupuncture to TE5 of left hand in normal subjects. *Am J Chin Med* 39(4):673–686
- Kiyimik MK, Güler I, Dizibüyük A, Akin M (2005) Comparison of STFT and wavelet transform methods in determining epileptic seizure activity in EEG signals for real-time application. *Comput Biol Med Trans* 35(7):603–616
- Lee YJ, Zhu YS, Xu YH, Shen MF, Zhang HX, Thakor NV (2001) Detection of non-linearity in the EEG of schizophrenic patients. *Clin Neurophysiol* 112(7):1288–1294
- Luo XL, Wang J, Han CX, Deng B, Wei XL, Bian HR (2012) Characteristics analysis of acupuncture electroencephalograph based on mutual information Lempel-Ziv complexity. *Chin Phys B* 21(2):561–568
- Mallat S (1999) A wavelet tour of signal processing, 2nd edn. Academic Press, San Diego
- Marwan N, Meinke A (2004) Extended recurrence plot analysis and its application to ERP data. *Int J Bifurc Chaos* 14(2):761–771
- Marwan N, Groth A, Kurths J (2007) Quantification of order patterns recurrence plots of event related potentials. *Chaos Complex Lett* 2(2/3):301–314
- Michel CM, Lehmann D, Henggeler B, Brandeis D (1992) Localization of the sources of EEG delta, theta, alpha, and beta frequency bands using the FFT dipole approximation. *Electroencephalogr Clin Neurophysiol* 82(1):38–44
- NIH consensus conference (1998) Acupuncture. *J Am Med Assoc* 280:1518–1524
- Onton J, Delorme A, Makeig S (2005) Variability of frontal midline EEG dynamics during working memory. *Neuroimage* 27(2):341–356
- Ouyang GX, Li XL, Dang C, Richards DA (2008) Using recurrence plot for determinism analysis of EEG recordings in genetic absence epilepsy rats. *Clin Neurophysiol* 119:1747–1755
- Paraskeva A, Melemenis A, Petropoulos G, Siafaka I, Fassoulaki A (2004) Needling of the extra 1 point decreases BIS values and preoperative anxiety. *Am J Chin Med* 32(5):789–794
- Ritter P, Moosmann M, Villringer A (2009) Rolandic alpha and beta EEG rhythms' strengths are inversely related to fMRI-BOLD signal in primary somatosensory and motor cortex. *Hum Brain Mapp* 30(4):1168–1187
- Rosso OA, Blanco S, Yordanova J, Kolev V, Figliola A, Schürmann M, Basar E (2001) Wavelet entropy: a new tool for analysis of short duration brain electrical signals. *J Neurosci Methods* 105(1):65–75
- Rosso OA, Martin MT, Figliola A, Keller K, Plastino A (2006) EEG analysis using wavelet-based information tools. *J Neurosci Methods* 153(2):163–182
- Stam CJ, van Woerkom TC, Pritchard WS (1996) Use of non-linear EEG measures to characterize EEG changes during mental activity. *Electroencephalogr Clin Neurophysiol* 99(3):214–224
- Stux G, Hammerschlag R (2001) Clinical acupuncture: scientific basis. Springer, Heidelberg

- Sutton S, Braren M, Zubin J, John ER (1965) Evoked potential correlates of stimulus uncertainty. *Science* 150(3700):1187–1188
- Takens F (1981) Detecting strange attractors in turbulence. In: Rand DA, Young LS (eds) *Dynamical systems and turbulence*. Lecture Notes in Mathematics, p 336
- Tyvaert L, LeVan P, Dubeau F, Gotman J (2009) Noninvasive dynamic imaging of seizures in epileptic patients. *Hum Brain Mapp* 30(12):3993–4011
- Zhang WT, Jin Z, Luo F, Zhang L, Zeng YW, Han JS (2004) Evidence from brain imaging with fMRI supporting functional specificity of acupoints in humans. *Neurosci Lett* 354(1):50–53